

Experimental investigation of local damage in high strength concrete columns using a shaking table

Rogério Bairrão†

*Structures Department, National Laboratory for Civil Engineering,
Av. Brasil 101, 1700-066 Lisboa, Portugal*

Rimantas Kačianauskas‡ and Romualdas Kliukas‡†

*Department Strength of Materials, Vilnius Gediminas Technical University,
11 Saulėtekio Ave, 10223 Vilnius-40, Lithuania*

(Received February 5, 2004, Accepted November 9, 2004)

Abstract. In this paper the accumulation of local damage during the cyclic loading in reinforced high-strength concrete columns is experimentally investigated. Two identical column specimens with annular cross-section and spiral reinforcement were designed and two tests, up to failure, under the action of a constant vertical concentrated force and a time-dependent concentrated horizontal force, were carried out at the LNEC shaking tables facility. Sine type signals, controlled in amplitude, frequency and time duration were used for these experiments. The concept of local damage based on local stiffness degradation is considered in detail and illustrated by experimental results. The specimens were designed and reinforced in such a way that the accumulation of damage was predicted by dominating deformations (cracking and crushing of the concrete) while the increasing of the loading values was a dominating factor of damage. It was observed that the local damage of HSC columns has exposed their anisotropic local behaviour. The damage accumulation was slightly different from the expected in accordance with the continuum damage concept, and a partial random character was observed.

Key words: high-strength reinforced concrete; column specimen; shaking table; local damage; stiffness degradation.

1. Introduction

In the 1980's, a new kind of concrete, namely, the high strength concrete (HSC) appeared in several countries and started to be applied in construction. Generally, the classification of concrete is used from the basic feature of concrete, which is its compressive strength f_c . Despite insignificant differences in various classifications, the HSC is characterized by the values of compressive strength $f_c = 60 - 150$ MPa. In parallel, a notion of high performance concrete (HPC) is introduced to emphasize other properties apart from the compressive strength. Major features of this concrete are

† Ph.D.

‡ Professor, Corresponding author, E-mail: rkac@fm.vtu.lt

‡† Associate Professor

porosity, absorbability, durability, freeze resistance, carbonization, etc., leading to high resistance in aggressive environment.

The transition from a conventional concrete to HSC and HPC was achieved due to special very fine aggregates such as silica fume and super-plasticizers. These additives are usually produced on the base of natural resources and industrial wastes different in every country. The effects of silica fume as an admixture reviewed in terms of mechanical and other properties may be found in de Larrard (1992), de Larrard and Puch (1992), Vadluga *et al.* (2000), Chung (2002), while effect of super-plasticizers on the properties of cement paste in Aitkin (1992), Heikal and El-Didamony (2000). In Portugal is being used a very fine addition produced in the North of the country. It is a by-product from the manufacture of silicon metal, with a silica content of 95%, which is used without any previous treatment.

The potential applications of HSC are almost limitless. During the last two decades research into the strength concrete developed rapidly and its application in construction has expanded greatly. Many bridges, tunnels, highways, multistory buildings, lighthouses, even nuclear power stations have been constructed using this material. The columns of hollow circular cross-section with longitudinal and spiral reinforcement under the action of combined vertical and horizontal loading, investigated in this paper, are among the structural members widely used in the construction of the above mentioned structures. A comprehensive review in the state-of-the-art of technology development and potential areas of application may be found in FIP/CEP (1990), Malier (1992), Flaga (2000), Kmita (2000).

The design of reliable high-quality engineering structures requires the understanding of their mechanical behaviour. Some of the characteristic features of HSC are a greater brittleness and a lower relation of tensile strength to compressive strength, which can cause a specific structural damage.

The damage phenomenology of reinforced HSC structures is still a non-completely resolved issue remaining a target of many investigations. The concept of damage and a theoretical background of the continuous damage mechanics (CDM) was probably first introduced in the pioneering work of Kachanov (1958) and is, essentially, of a phenomenological nature. Continuum damage, generally speaking, can be interpreted as the decay of mechanical properties with increasing stress and/or strain. CMD, for example Lemaitre and Lipman (1996), has proved to be a systematic and promising approach to the analysis and fracture for a wide variety of materials. It was also proved that damage mechanics-based models have been able to accurately account for the microcracking and softening behaviour of conventional concrete. For this purpose, a number of irreversible thermodynamics theories of CDM also coupled with plasticity have been developed and applied (Suanno and Ramm 1994, Papa and Taliercio 1996).

The HSC possess, however, anisotropic elastic-brittle damage behaviour while several models aimed to modify the constitutive equations and the damage evolution laws appeared to describe the accumulation of damage for different loadings in the framework of CDM (Murakami and Kamiya 1997, Khan *et al.* 1998, Li *et al.* 2002).

The accumulation of damage is a process lasting during the whole period of operation until a critical state (failure) of the structure is reached. However, the degree of degradation of the elastic continuum, defined by CDM models, describes the state of the material, on a point by point basis, which can not be easily extrapolated to the entire structure and does not allow us to conclude about the capacity level of the damaged structure to withstand the loading. As a result, it may be stated that the change of the global behaviour depends on many factors and may be heavily predefined by

local damage, where the location and size of the processing zone play an important role. A comprehensive review of the local/global damage concepts and discussion may be found in Hanganu *et al.* (2002).

In spite of the existence of theoretical concepts and numerical methods to evaluate the actual behaviour of damaged structures, experimental testing still remains the most powerful and reliable research tool. The main reason is that actual behaviour of the material depends on the scale of specimens or processing zones. It must be stated, however, that the experimental research is progressing at a rate much more slower than the theoretical one. The lack of experimental data is a serious drawback in the evaluation of the reliability of the proposed theoretical models, when applied to structural members.

Many experimental studies concerning fracture and damage behaviour and properties actually belong to the set of mechanical small-scale laboratory tests. An illustration of such experiments on HSC damage under static monotonic or cyclic loading may be found in Murakami and Kamiya (1997), under cyclic bending in Manfredi and Pecce (1997) and under triaxial cyclic compression in Li *et al.* (2002). The application of acoustic emission to monitor the evolution of damage in very high strength specimens is presented by Labuz *et al.* (2001).

The detection of the accumulation of damage may be also resolved through dynamic experiments, but the experimental investigation of large-scale structural members, especially under the action of dynamic loading, is much more complicated. Therefore, the majority of column experiments have been performed under static loading. Some examples of experimental research on HSC columns may be found in Foster (2001) and Paultre *et al.* (2001).

Recently, various advanced and innovative experimental techniques, using computer-controlled displacements have provided a basis for realistic dynamic simulation. Damage detection from the measured natural frequencies is probably among the simplest dynamic experiments (Zhu *et al.* 2003). The shaking table testing started its development in the early fifties and still remains an essential tool for investigating structures under dynamic loading, since it allows the study of true inertia forces affecting the specimens. Several shaking tables throughout the European Union (Crewe and Severn 2001), as well as in USA (Conte and Trombetti 2000), and Japan (Ogawa *et al.* 2001), are being used to develop research activities about the dynamic effects on civil engineering structures. However, the models tested by the shaking tables are normally constructed at a reduced scale, therefore, testing capabilities are restricted to structural members or small-scale fragments, unless very important shaking tables are used. Experimental investigations of the global damage and failure of reinforced columns with the use of a shaking table are presented by Minowa *et al.* (1995) and Lu (1995). A realistic damage of reinforced concrete bridge piers, during the Northridge earthquake, paying special attention to flexure-shear-axial interaction was demonstrated by Lee and Elnashai (2002).

An advanced triaxial shaking table was also designed and built in the Portuguese National Laboratory for Civil Engineering (LNEC) in Lisbon (Emílio 1989, Duarte 1994, Bairrão *et al.* 1995). It consists of a large rectangular platform (or table) that is driven in up to six degrees of freedom, where the test specimens are fixed and shaken.

The current experimental investigation of the local damage in reinforced HSC columns under horizontal and vertical loading was carried out at the LNEC shaking tables facility. Two identical column specimens V1 and V2, with annular cross-section and spiral reinforcement, were designed and two tests, up to failure, under the action of a constant vertical concentrated force and time-dependent concentrated horizontal force were carried out. The investigation of the global damage of

the HSC column is presented in Bairrão *et al.* (2003), while a concept of the investigation of the local damage has already been briefly reported by the authors Bairrão, Kačianauskas and Kliukas (2003).

The local behaviour and accumulation of the local damage during the cyclic loading is considered mainly in the present paper. The construction of the specimens, set-up of experiments and the measured forces and displacements are presented. A concept of the local damage based on the local stiffness degradation is considered in detail. Finally, the accumulation of the local damage and a comparison of the damage index in different local zones is illustrated and discussed.

2. Data of the column specimen

Two identical reinforced HSC column specimens, V1 and V2, with circular hollow cross-section and spiral containment were designed and built at LNEC in Lisbon. The entire specimens were produced as monolithic units consisting of a massive footing and a specified column. The geometry and cross-section details of the test specimen are illustrated in Fig. 1. The length of the column was 215 cm, the diameter - 26 cm and the wall thickness - 6 cm. Specimens did contain special holes, voids and stiffening details necessary for the application of external loads and for insuring testing conditions.

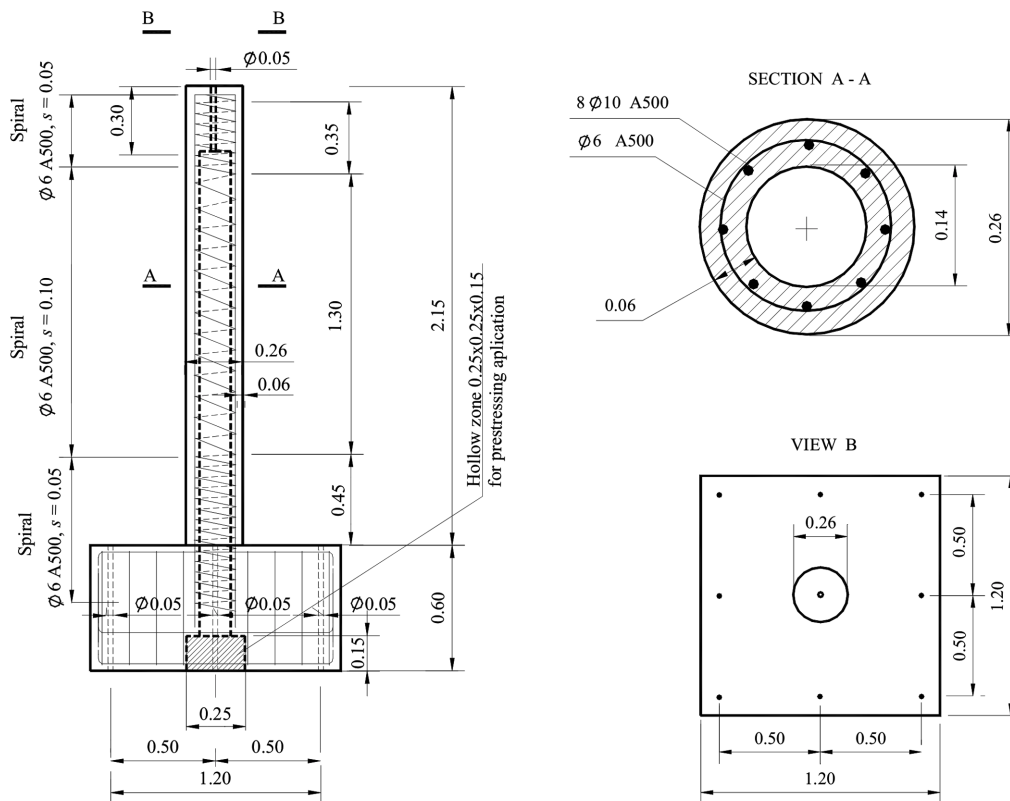


Fig. 1 Geometry and cross-section details of the test specimen

Table 1 Composition of the high-strength concrete

Basic ingredients	Quantity (kg)	Notes
Gravel	876	
Sand	864	
Cement	450	
Silica fumes	50	Produced in Portugal
Addendum G51	10	About 2% of the cement mass
Water	130	Water/Cement relation ≈ 0.29

The composition of the concrete used for the columns was specified with the specimen of $10 \times 10 \times 10$ cm in order to achieve a cubic compressive strength of about 80 MPa. The main data of this composition used for producing one cubic meter of the high-strength concrete is presented in Table 1.

The mechanical properties of the concrete used for columns were evaluated by standard compression tests, performed on a series of cubic and cylindrical probes. The testing results confirmed the expectation and provided a good value of compressive strength $f_c = 82$ MPa. According to recommendations given by Dong and Keru (2001), the elasticity modulus of HSC may be calculated from compression strength as

$$E_c = 10^4 \cdot f_c^{1/3}$$

providing the value of $E_c = 43.6$ GPa.

Longitudinal reinforcement consisted of 8 bars of 10 mm in diameter, while the containment was a spiral made up with 6 mm diameter with different bar spacings s (Fig. 1). The steel was defined by a strength value of 500 MPa, while the elasticity modulus of the reinforcement was $E_s = 200$ GPa.

3. Testing procedure and setup

Two tests up to failure were carried out at the LNEC shaking tables facility. The tested column is considered as a vertical cantilever beam of length L loaded by combined vertical and horizontal actions. A vertical load $N = 187.5$ kN, producing the axial force, was applied before testing and remained constant during the entire testing period. It was implemented by pre-stressing a cable positioned inside the column, at its central line, and connected from the top of the column to a hollow zone under the footing.

LNEC shaking table used for testing is a very particular simulator having three independent translation degrees of freedom, which are driven by hydraulic actuators, whereas its rotational degrees of freedom are minimized by torque tube systems, one for each axis (roll, pitch and yaw). Under the horizontal cranks a system of passive gas actuators compensates for the dead weights of the shaking table and of the testing specimen or, if needed, a set of removable rigid blocks eliminate absolutely the vertical motion of the table.

The main characteristics of this shaking table are an area of $5.6 \text{ m} \times 4.6 \text{ m}$, a table mass of about 40 t, a maximum allowable specimen weight of 400 kN, a frequency range from 0 to 15 Hz, maximum accelerations of 1.1, 0.5 and 1.8 g for the transverse, vertical and longitudinal axes,

respectively, and maximum displacements of ± 175 mm simultaneously for all the three axes. Detailed information on the characteristics of the shaking table can be found in Emílio (1989).

The horizontal time-dependent loading was produced by the imposition of a shaking table motion and by the action of an inertia mass involving a set of external masses and a connecting rod. This set was connected to an L -shaped steel structure laying on Teflon pads which were attached on the top of a fixed supporting structure located outside the shaking table. The L -shaped structure together with the attached mass was presumed to be able to slide over the supporting structure with very low friction forces. The connection of this rod to the ring and to the L -shaped structure was made with spherical swivels, thus allowing free rotations in all directions. Finally, the total value of the external mass was $m = 12$ t. A general view of the setup is shown in Fig. 2.

The motion of the shaking table was prescribed as a function of the controlled transverse horizontal time-dependent displacement $u_{tab}(t)$. A schematic illustration of testing is presented in Fig. 3.

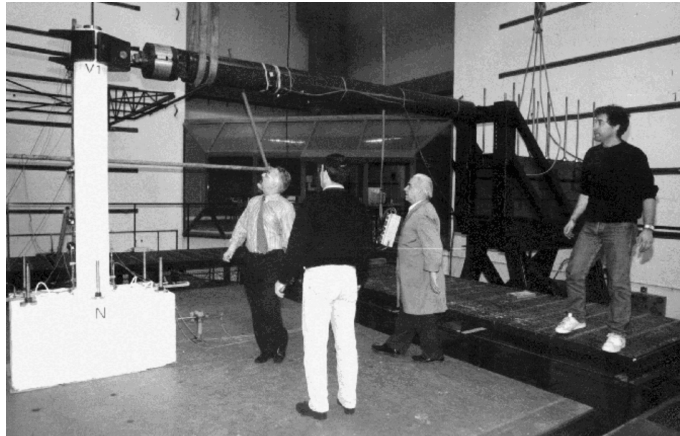


Fig. 2 Test setup

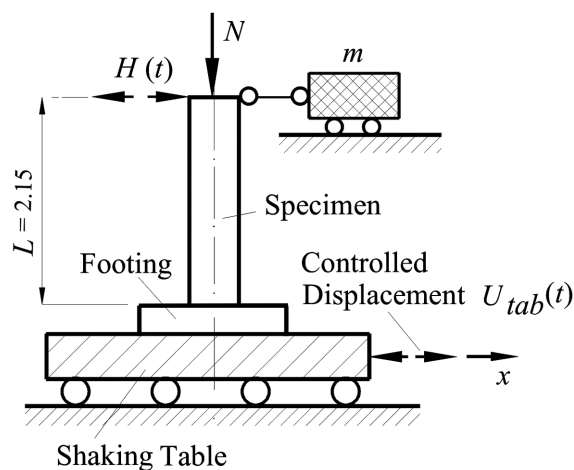


Fig. 3 Schematic illustration of testing

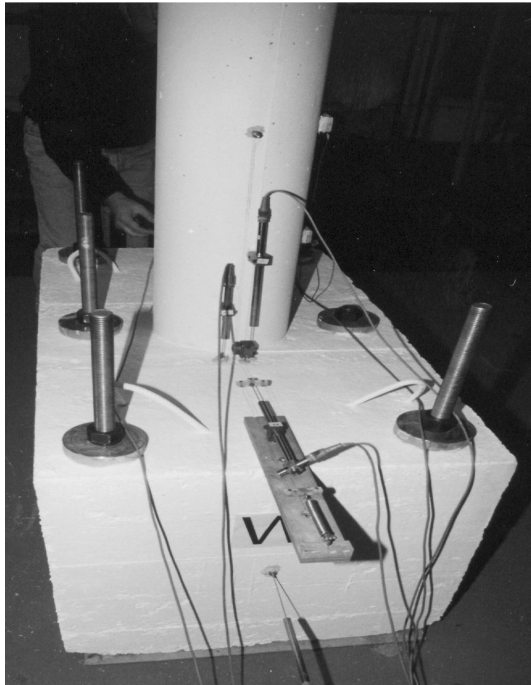


Fig. 4 Detail of the displacement transducers on the specimen

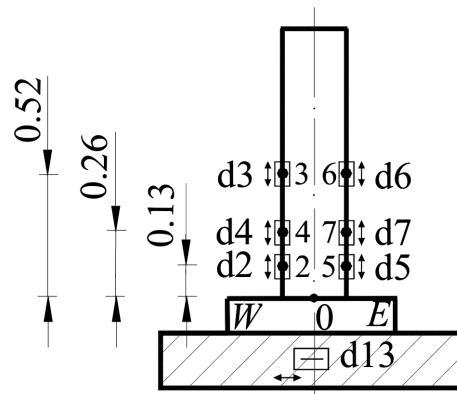


Fig. 5 Location of the displacement transducers

In testing, the movement of the shaking table in the transverse direction was measured by the optical transducer d13. The horizontal force $H(t)$, generated at the top of the column, was measured directly by a loading cell, inserted as part of the connecting rod between the specimens and the inertial mass.

In order to monitor the local damage, the vertical (longitudinal) displacements of the prescribed points 2, 4 and 3 located on the W side and 5, 7 and 6 located on the E side were registered. The local zones 0-2, 2-4 and 4-3 on the W side and 0-5, 5-7 and 7-6 on the E side are characterized by the respective lengths $L_{0-2} = L_{0-5} = 130$ mm, $L_{2-4} = L_{5-7} = 130$ mm and $L_{4-3} = L_{7-6} = 260$ mm. The vertical displacements with respect to a column footing were measured by the inductive displacement transducers d2 to d7. A general view of the transducers on the specimen is presented in Fig. 4, while their location is schematically illustrated in Fig. 5.

4. Experimental results

For these experiments, sine type signals, controlled in amplitude, frequency and time duration, were used. The loading history is separated into six stages denoted as S1 - S6. The data of loading for specimen V1 at each stage are given in Table 2, while the data of loading for specimen V2 are given in Table 3.

The measured experimental data for specimens V1 and V2 may be described as follows. The time variation of the acquired controlling displacement of the shaking table $u_{tab}(t)$ during all stages from

Table 2 Loading data for specimen V1

Stage	Displacement amplitude u_{tab} (mm)	Excitation frequency (Hz)	Duration time (s)	Type of the loading
S1	6.3	2.0	20	Sine wave
S2	9.5	2.0	20	Sine wave
S3	12.7	2.0	20	Sine wave
S4	23.0	1.4	20	Sine wave
S5	36.0	0.9	20	Sine wave
S6	32.0	1.0 to 0.1	150	Sine-sweep

Table 3 Loading data for specimen V2

Stage	Displacement amplitude u_{tab} (mm)	Excitation frequency (Hz)	Duration time (s)	Attack time (s)	Type of the loading
S1	6.3	3.0-1.0	20	none	Sine-sweep
S2	8.0	2.0	20	10	Sine wave
S3	12.7	2.0	20	10	Sine wave
S4	23.0	1.4	20	10	Sine wave
S5	36.0	0.9	20	5	Sine wave
S6	32.0	1.0 to 0.1	150	none	Sine-sweep

S1 to S6 is shown in Fig. 6. The global response of the specimen may be characterized by the horizontal force $H(t)$, time variation of which is shown in Fig. 7.

As can be seen in the graph, the input signal of displacement of the shaking table $u_{tab}(t)$ was designed differently for each of the specimens, resulting, consequently, in a different character of the load $H(t)$.

For the specimen V1 the input signal was imposed like it is commonly used in cyclic fatigue tests. The controlled displacement of the shaking table $u_{tab}(t)$ at the stages from S2 to S5 during the whole active interval (between 2.5 and 22.5 sec) was designed as a sine wave with constant amplitude, which generally produces a global response of the structure as a stable sine wave motion. The examination of the character of the force $H(t)$ amplitudes proves that the mass m of the structure becomes to be active in the starting phase of motion.

For the specimen V2 the input signal was imposed in a way used in cyclic accumulation tests. The controlled displacement of the shaking table $u_{tab}(t)$ was designed as a sine wave having a progressively increasing amplitude during the first attack phase (the interval between 2.5 and 12.5 sec) and a constant amplitude during the second phase (the interval between 12.5 and 22.5 sec). As a result, the external mass m became to be active only in the second phase of motion.

In order to observe the behaviour of the specimens after critical accumulation of the local damages and the final failure, at the stage S6 the tests were performed in a different way. Here, the controlled displacement of the shaking table $u_{tab}(t)$ for both specimens was designed as a sine-sweep signal having a progressively decreasing frequency. During the period of loading, lasting 40 seconds for specimen V1 and 70 seconds for specimen V2, the inertia effect produced increasing load amplitudes, while the column was still able to resist the external load. The remainder period is

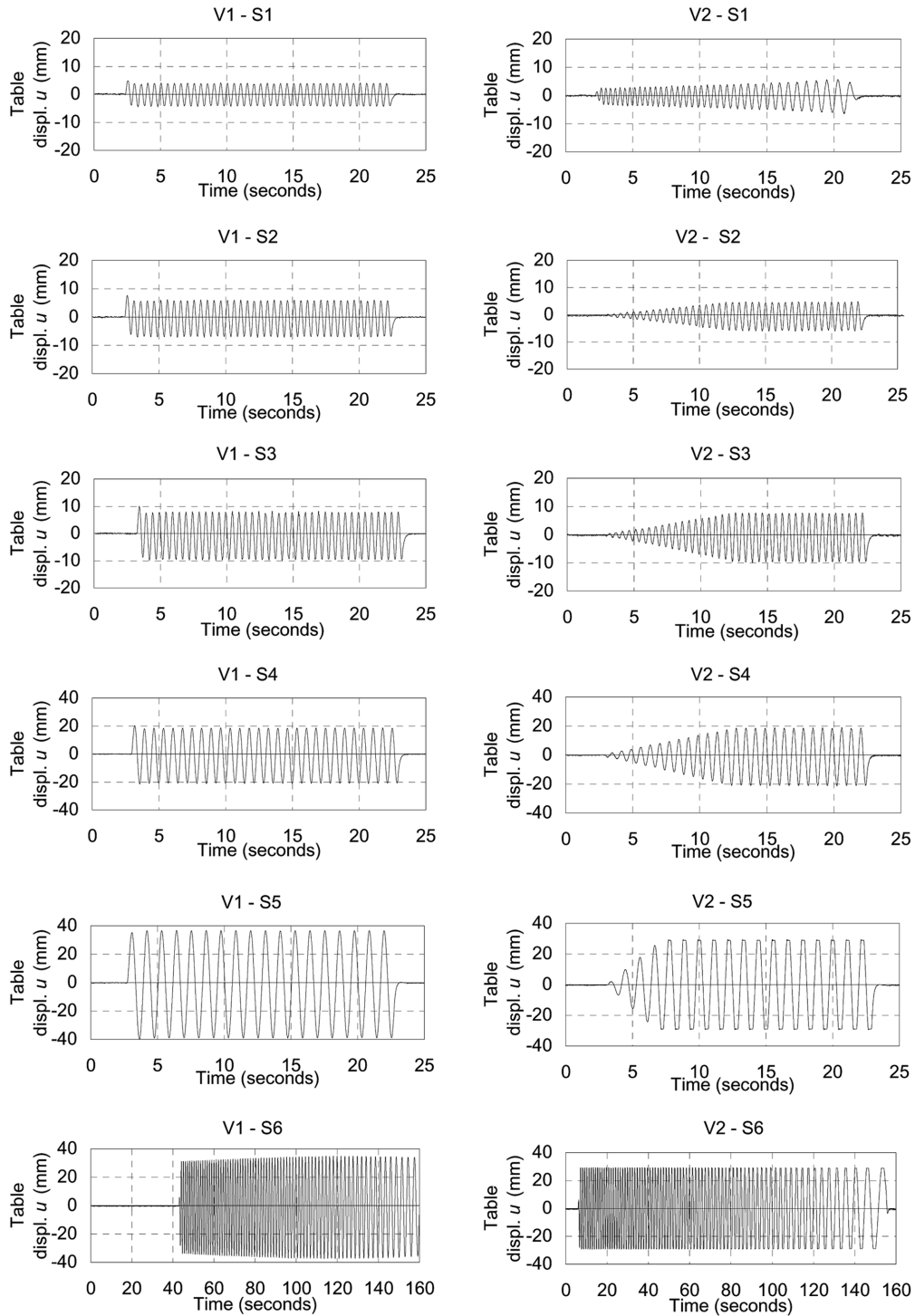


Fig. 6 Time histories of the shaking table $u_{tab}(t)$ displacements

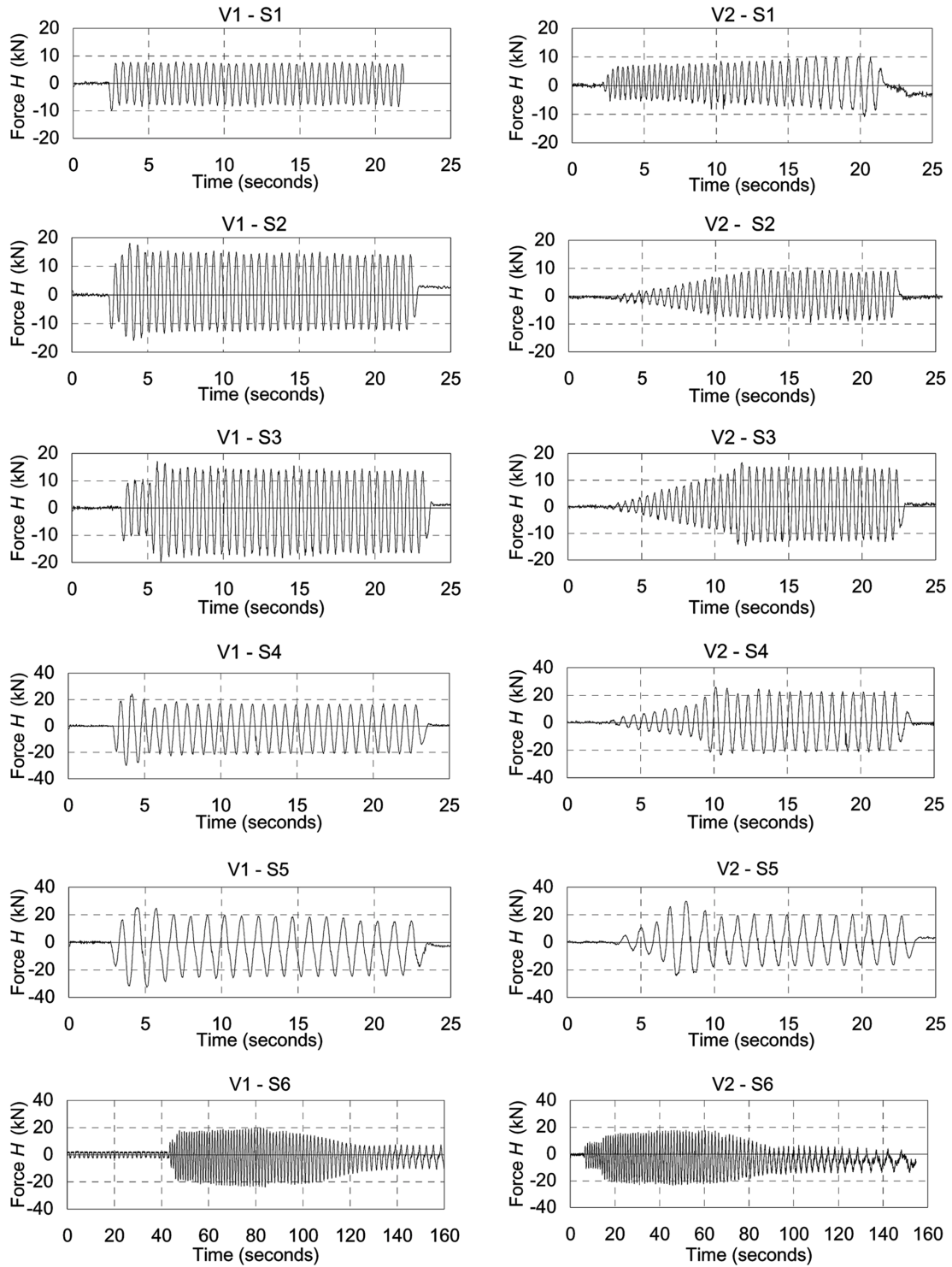


Fig. 7 Time histories of the horizontal load $H(t)$

characterized by the occurrence of several cracks and total crushing of concrete, which lead to a decrease of the load amplitudes indicating the final failure.

5. Damage concept

The damage concept employed here to investigate the accumulation of damage is mainly associated with the conventional approach used in continuum damage mechanics, assuming that it is possible to establish an evolution law of damage at each point of the structure. The term ‘local damage’ applied here, does not refer to an individual point but rather to the local processing zone of a finite size. It may be considered as a certain extension of the continuum approach, which seems to be preferable for non-homogeneous anisotropic materials or structural members, where geometry, construction and many other indirect factors are of major importance.

By applying the definitions used in continuum damage mechanics, the local axial stiffness $K_{i-j}(t)$ may be considered as the damage indicator for bending. The effective local stiffness of the local processing zone $i - j$ at time t , the decreasing of which results basically in the increasing of the damage may be expressed as follows:

$$K_{i-j}(t) = K_{\max i-j}(1 - d_{i-j}(t)) \tag{1}$$

Expression (1) describes the degradation of stiffness of the local processing zone compared to the stiffness value $K_{\max i-j}$ at the virgin state. The scalar variable $d_{i-j}(t)$ ($0 \leq d_{i-j}(t) \leq 1$) is referred to as a local damage index, being defined in the traditional manner as

$$d_{i-j}(t) = \frac{K_{\max i-j} - K_{i-j}(t)}{K_{\max i-j} - K_{\min i-j}} \tag{2}$$

The effective local stiffness $K_{i-j}(t)$ ($K_{\min i-j} \leq K_{i-j}(t) \leq K_{\max i-j}$) may be calculated as the tangent of the experimentally obtained loading curve

$$K_{i-j}(t) = \frac{|H(t)|}{|e_{i-j}(t)|} \tag{3}$$

where $H(t)$ stands for the global force, while $e_{i-j}(t)$ is a relative local elongation of the external layer of the local zone. The validity of expression (3) is restricted in the vicinity of a zero displacement $u(t) \approx 0$, where $K_{i-j}(t)$ tends to infinity.

The relative local elongation may be obtained from the measurements as a relative difference of displacements at points i and j :

$$e_{i-j}(t) = (u_j(t) - u_i(t))/L_{i-j} \tag{4}$$

where L_{i-j} is the length of the local processing zone.

Actually, normalization of the scale for damage accumulation is a complicated task because exact evaluation of the stiffness limits $K_{\max i-j}$ and $K_{\min i-j}$ is based on rather heuristic considerations. In

any case, damage accumulation (2) will be presented in a relative scale, remaining independent of normalization parameters.

In the current presentation, the local stiffness means the horizontal force due to a unit local strain. Generally, it is a position-dependent variable defined by the distance y between the horizontal force and the centre of the local processing zone. Assuming elastic damaged concrete obeying Hook's law, the local elongation may be considered as a strain $e = \sigma/E$ and expressed using the formula for the case of an elastic cantilever beam

$$e_{i-j}(y) = \frac{Hy_r}{EI} \quad (5)$$

where I is a modified moment of inertia of the composite section taking into account the elasticity properties of both concrete and reinforcement, also including spiral reinforcement, and r being the section radius.

Finally, by inserting Eq. (5), into expression (3), the local stiffness may be presented explicitly. For the limit stiffness of the local zone $i-j$ it may be summarised in the following manner:

$$K_{\max(\min) i-j} = \frac{E_{\max(\min)} I_{\max(\min)}}{y_{i-j} r} \quad (6)$$

where $E_{\max(\min)}$ presents the limit values of the secant modulus of the homogeneous material, $I_{\max(\min)}$ – limit values of an axial inertia moment of the section in the limit state and y_{i-j} – the distance between the horizontal force and the centre of the local processing zone.

The maximal value of the stiffness $K_{\max i-j}$ is expected to correspond to the virgin elastic stiffness. At this stage, the elasticity modulus E_{\max} corresponds to the elasticity modulus of the concrete $E_{\max} = E_c$, while the inertia moment $I_{\max} = I_{\max}(E_c)$ is a modified moment of the virgin section.

The substitution of the values of the elasticity modulus $E_c = 43.6$ GPa and $E_s = 200$ GPa and the geometric data of cross-section (Fig. 1) yields the value $I_{\max} = 217.8 \cdot 10^{-6} \text{ m}^4$. The position of local zones is defined by distances (Fig. 5) $y_{0-2} = y_{0-5} = 2035$ mm, $y_{2-4} = y_{5-7} = 1905$ mm and $y_{4-3} = y_{7-6} = 1710$ mm. Finally, according to Eq. (6), the virgin elastic stiffness is defined by the following values: $K_{\max 0-2} = K_{\max 0-5} = 35733$ kN, $K_{\max 2-4} = K_{\max 5-7} = 38172$ kN and $K_{\max 4-3} = K_{\max 7-6} = 42525$ kN.

As proved by the experimental results, in particular by those presented in Fig. 7, the critical damage of the specimens is reached at the end of stage S5 by the occurrence of through-crack and final crushing of concrete at the footing. The minimal limit stiffness of the local zone at failure is merely predefined by the stiffness of longitudinal reinforcement. According to (BAEL91 Regulation), the limit strain of reinforcement has to be taken as $\varepsilon_s = 10^{-3}$. Now, the elasticity modulus of the reinforcement is taken as its secant elasticity modulus. It is evaluated from the stress-strain diagram by inserting the strain value. It takes the value $E_{\min} = 54.5$ GPa, while $I_{\min} = 3.11 \cdot 10^{-6} \text{ m}^4$ is the axial inertia moment of reinforcement. Finally, the stiffness at failure was defined by the values $K_{\min 0-2} = K_{\min 0-5} = 926$ kN, $K_{\min 2-4} = K_{\min 5-7} = 990$ kN and $K_{\min 4-3} = K_{\min 7-6} = 1103$ kN.

The proposed local damage concept applied to bending also encompasses non-linearity, three-dimensional effects, effects of axial loading and other indirect factors difficult to be extracted and decoupled from damage assessment. In spite of the above drawbacks, it seems to be a realistic tool to describe the accumulation pattern of HSC column specimens.

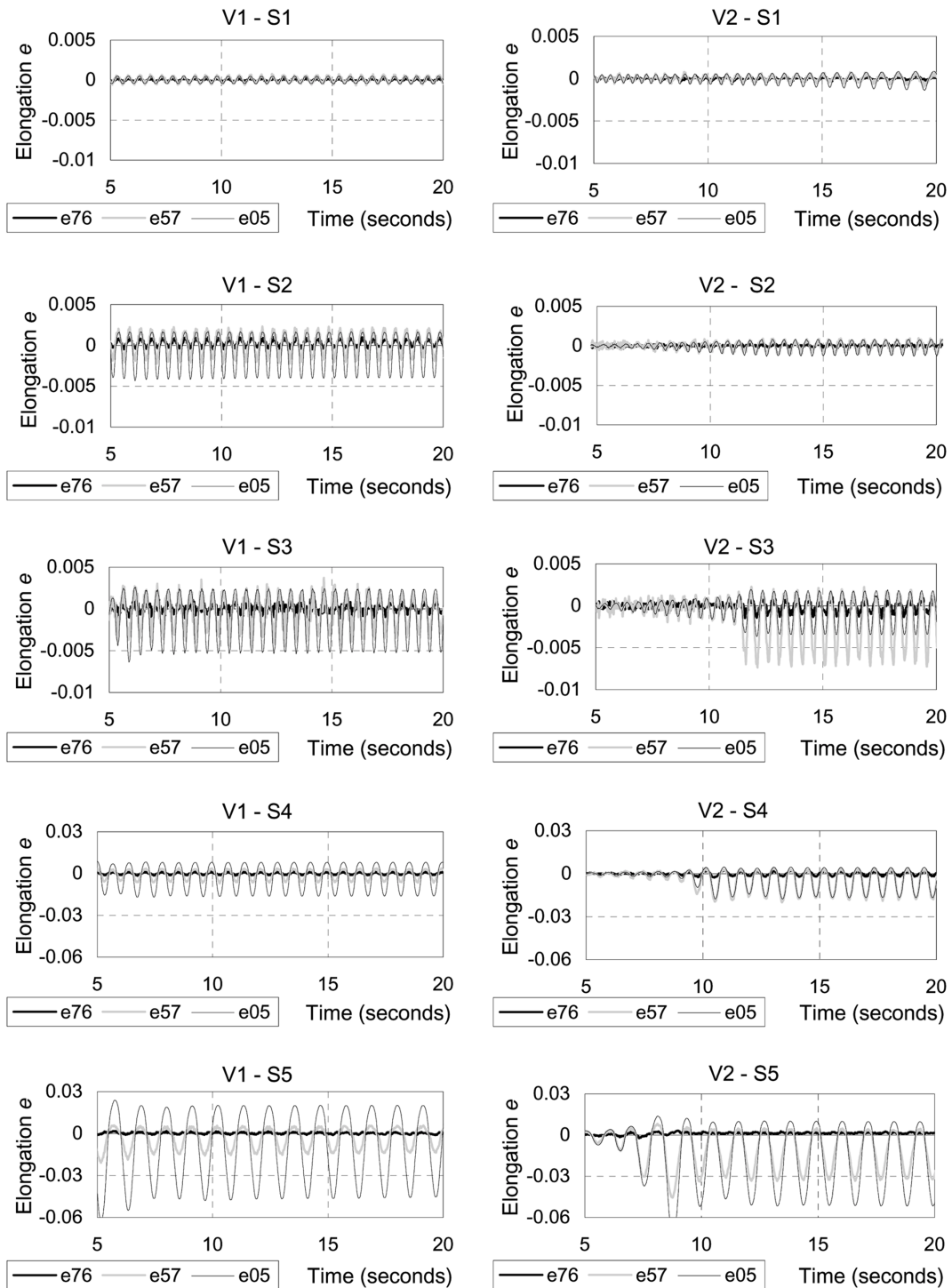


Fig. 8 Time histories of the local elongations e_{i-j} at side E

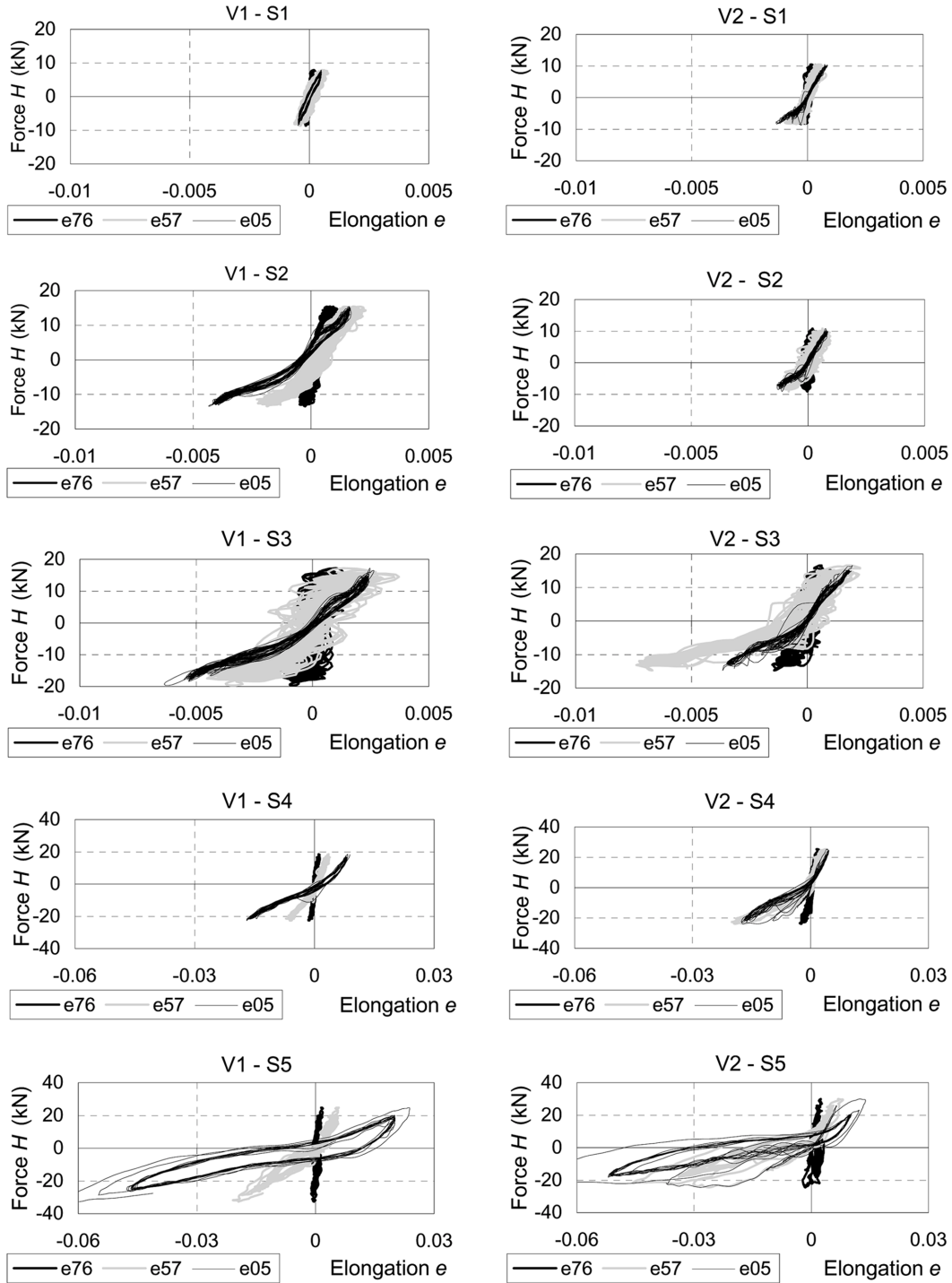


Fig. 9 Force-elongation diagrams at side E

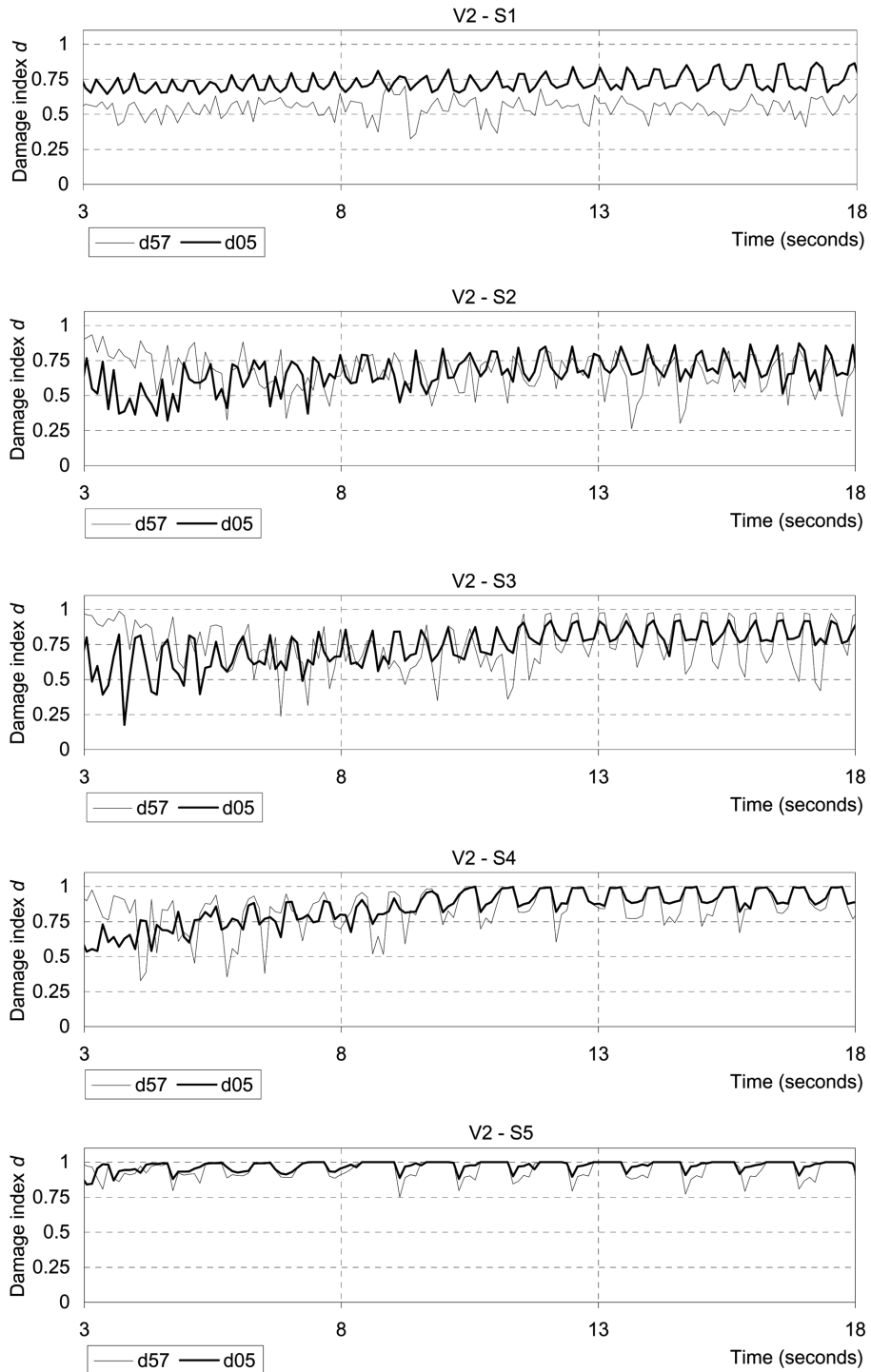


Fig. 10 Time histories of the local damage indices $d_{0.5}$ and $d_{5.7}$ for specimen V2

6. Investigation of damage

The accumulation of damage in reinforced HSC column specimens is a process lasting during the period of operation until the critical state (failure) of the structure is reached and encompasses stages S1 to S5. The time histories of the relative elongations $e_{0.5}(t)$, $e_{5.7}(t)$ and $e_{7.6}(t)$, on the side E for both specimens V1 and V2 required for evaluating of the local damage indices according to Eq. (2) and obtained by Eq. (4) are presented in Fig. 8. Hereafter, elongations in the figures are denoted by e05, e57 and e76. Finally, the local behaviour characterized by the corresponding force-strain curves $H(t)-e_{i-j}(t)$ is shown in Fig. 9.

Since the elongation in the local zone 4-3 and 7-6 varies insignificantly, the following investigation of damage is restricted to the most seriously damaged local zones at the bottom of the specimen. The time histories of the local damage indices $d_{0.5}$ and $d_{5.7}$ on the side E for the specimen V2 obtained by using the definitions (2)-(4) and after filtration are illustrated in Fig. 10. Hereafter, damage indices in the figures are denoted by d05, d57, etc. The presented graphs allow us to recover the pattern of damage accumulation during the entire loading period.

The results have proved that the critical damage accumulates mainly at the stages S4 and S5. The detailed comparison of damage indices on both sides of the specimens V1 and V2 is shown in Fig. 11 through Fig. 14, while the views of both specimens at the critical damage are presented in Fig. 15.

Based on experimental results, as well as on the observation of the behaviour of the damaged specimens, a general picture of the local damage accumulation may be recovered in the following manner. The specimen V1 at stage S1 and the specimen V2 at the stages S1 and S2 were subjected to a relatively low amplitude ($H_{\max} \leq 10$ kN) of an horizontal force. In spite of this, the tension stresses in concrete were beyond the tension resistance at this loading level and the development of microcracks was indicated by permanently increasing values of the damage index. The first cracks were closed and hardly observed after unloading due to the compression of a longitudinal load. The damage was also caused by local damage effects of different kind (due to disregard of the technological requirements of manufacture and testing set-up). However, the test setup and measurements were not sufficiently sensitive to follow accurately the elastic behaviour of concrete at low strain values, therefore, only the average stiffness values may be considered as a local damage indicator for low values.

At the stages S3 and S4, a dominant accumulation of damage has been observed. This phase is characterised by the occurrence and development of macrocracks and their changes in length and width. The relatively small 100 - 200 mm distances between the cracks indicate a quite perfect bond between concrete and reinforcement. For the most seriously damaged zones, the damage index has reached critical values. The accumulation of damage for the specimen V1 with strongly impulsive loading is related to higher load values at the beginning of each loading stage in the short period of attack time between 3 and 5 seconds. For the specimen V2 with permanently increasing loading amplitude the damage accumulation period lasts between 3 and 12 seconds. The damage diagrams illustrate the opening of macrocracks at 8 and 11.5 seconds during stage S3 on the E side. Finally, it can be proved by the variation of the damage index, that increasing of loading values was a dominating factor of damage.

In spite of the above relative regularity, the local damage of the HSC structure has accumulated in a different way from that expected by the continuum damage concept. The propagation of the local damage had, however, a random character caused by the effects of different sources such as the

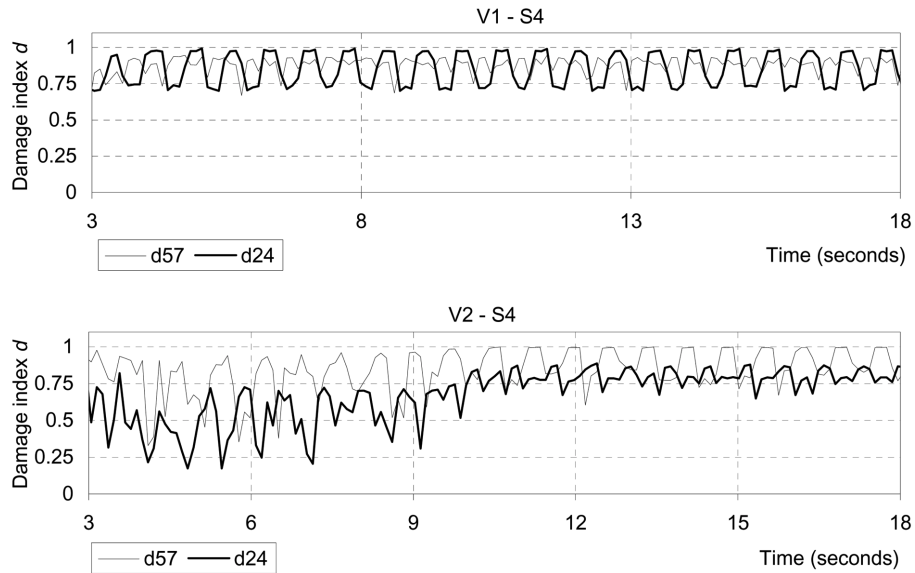


Fig. 11 Variation of the local damage indices $d_{2.4}$ and $d_{5.7}$ at stage S4

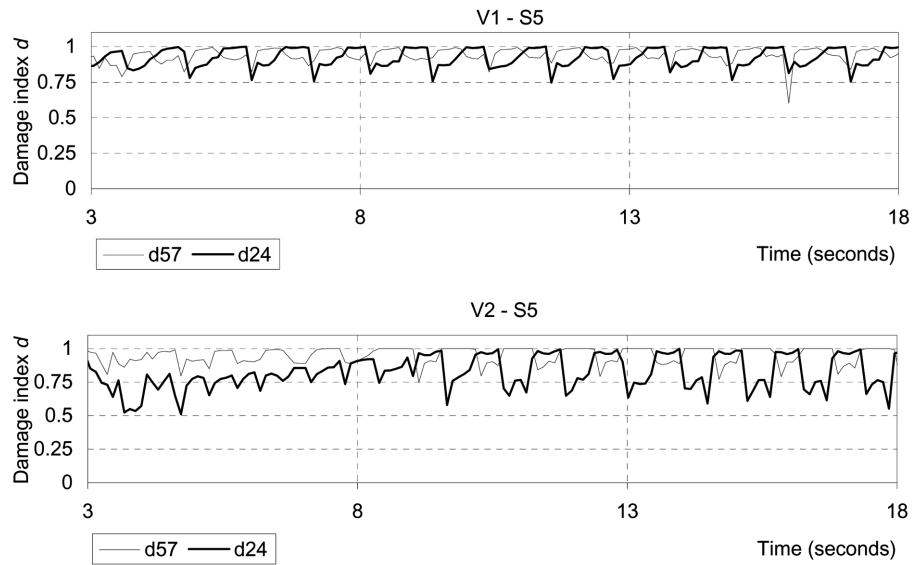


Fig. 12 Variation of the local damage indices $d_{2.4}$ and $d_{5.7}$ at stage S5

disregard of technological requirements of manufacture, non-homogeneity of the materials, etc. The random properties provide a non-symmetric bending behaviour of an apparently symmetric specimen with an average of 10 to 15% scattering of the local damage index when comparing the two sides of the columns. The opening of macrocracks on one side leads to different local damages, depending on compression or tension of the cracked side.

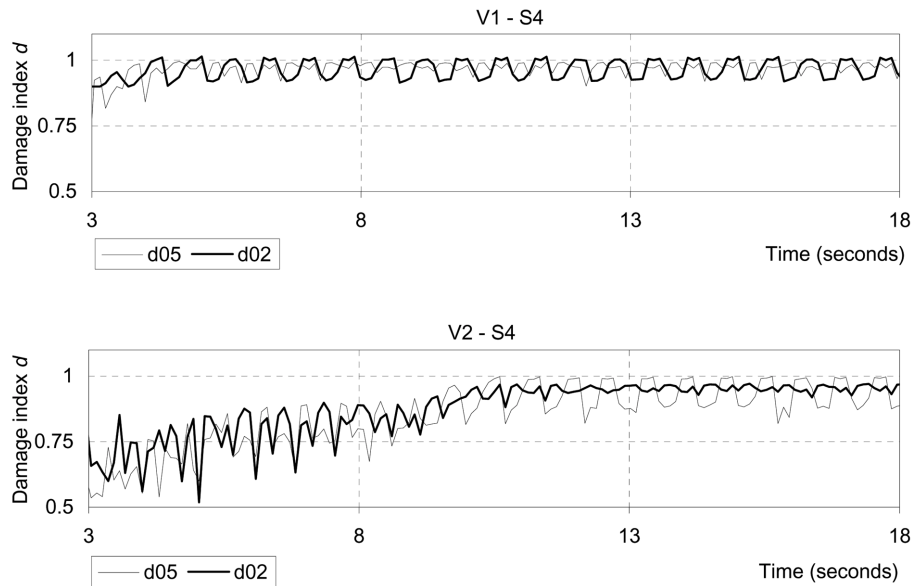


Fig. 13 Variation of the local damage indices $d_{0.2}$ and $d_{0.5}$ at stage S4

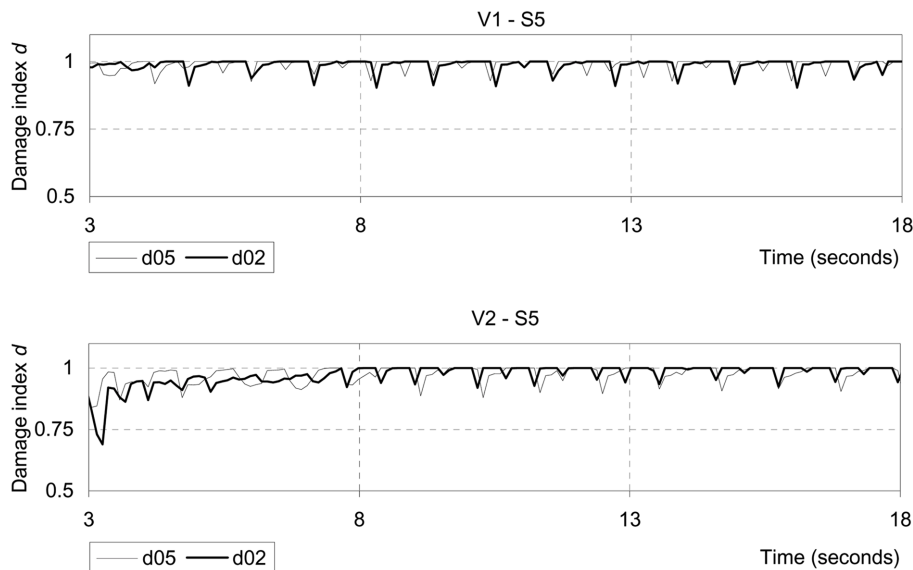


Fig. 14 Variation of the local damage indices $d_{0.2}$ and $d_{0.5}$ at stage S5

The variation of the local damage indices shown in Fig. 11 and Fig. 12 exposes the differences of zones 2-4 and 5-7, which are relatively distant from the footing. The damage remains, however, critical for tension but allowing the specimen to resist compression because of the axial load.

The random character of damage may provide considerable differences in the local processing zones, where a lower level loading leads to a higher than expected level damage. This phenomenon

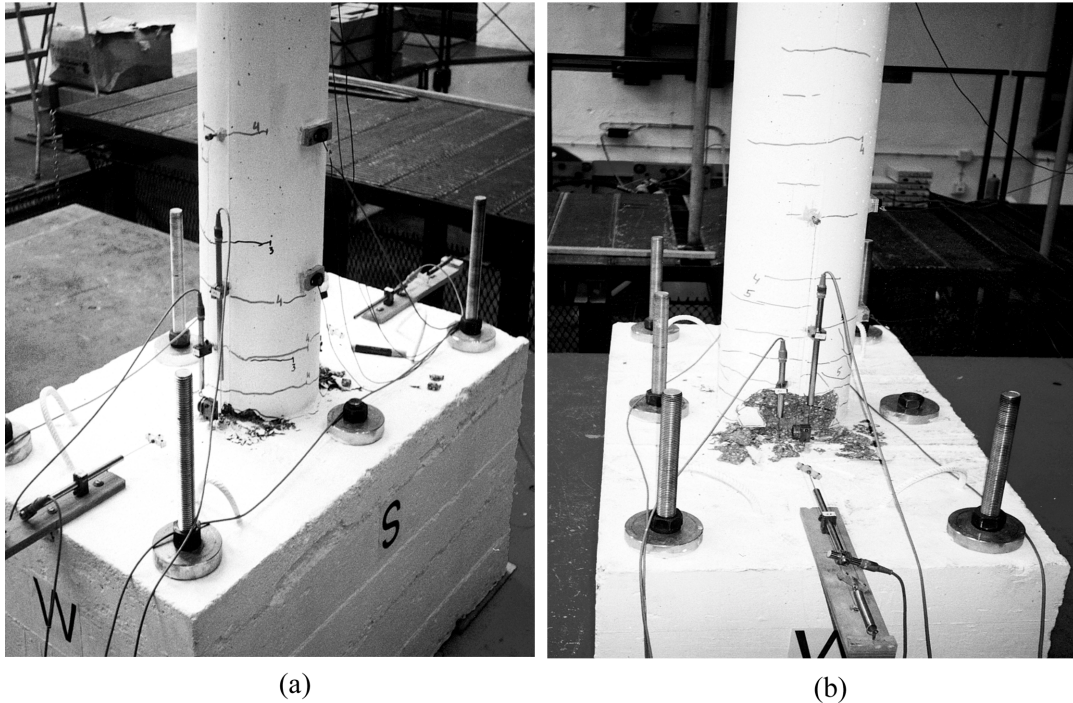


Fig. 15 Views of the specimens after the critical accumulation of damage at stage S5: (a) side W of the specimen V1, (b) side W of the specimen V2

has been observed in specimen V2 at stage S3 and is clearly indicated in Figs. 8, 9 and 10, where the occurrence of macrocracks in the local zone 5-7 is the main reason for an unexpected increase of the local damage index compared to zone 0-5.

The accumulation of damage became stable at stage S5, reaching its critical value in the local zones 0-2 and 0-5 at the bottom of the column on both sides E and W, but it was due to different reasons for each specimen. For the specimen V1 the damage accumulates, disconnecting the column from the footing. For the specimen V2 it is characterised by the development of the through-crack and final crushing of the column concrete at the footing.

7. Conclusions

After this shaking table investigation of the local damage in different processing zones of high-strength reinforced concrete columns, under horizontal and vertical loading, the following conclusions have been drawn:

- 1) The specimens under investigation were designed and reinforced in a way that the accumulation of damage could be predicted by the dominating deformations, cracking and crushing of the concrete.
- 2) The test setup and measurements of the vertical displacements adopted were capable to detect the local damage predefined by a high ratio of stiffness degradation. These measurements were,

however, not sufficiently sensitive to follow accurately the behaviour of the concrete during the very low damaged phase.

- 3) The increasing of loading values was a dominating factor of damage, which was proved by the variation of the damage index. The considerable accumulation of damage for the specimen V1 with strongly impulsive loading was related to higher load values at the beginning of each loading phase in the short period between 3 and 5 seconds. For the specimen V2, with permanently increasing loading amplitude, the damage accumulation period was mainly detected between 3 and 12 seconds.
- 4) The propagation of local damage in HSC had, however, a random character caused by the effects of different sources such as the disregard of technological requirements of manufacture, the non-homogeneity of the local zones, etc. Random factors provided a non-symmetric bending behaviour of an apparently symmetric specimen with an average of 10 to 15% differences in the local damage index between the opposite sides. Considerable differences in damage of the neighbouring processing zones located on the same side were also indicated. This kind of damage was caused due to occurrence of macrocracks observed in the local zone 5-7 with lower level loading compared to highly loaded zone 0-5 (specimen V2, stage S3).
- 5) Finally, it may be concluded, that the local damage of HSC structure produces anisotropic local behaviour and is accumulated in a discrete way, while the scattering observed is of a random character. The experimental results obtained may be helpful to validate constitutive damage models in future investigations.

Acknowledgements

A partial support for scientists from Central and Eastern European Countries by the European Community Program “Access to Large Scale Facilities – The Large Installations Plan”, in the framework of ECOEST, “European Consortium of Earthquake Shaking Tables” is acknowledged.

References

- Aitcin, P.C. (1992), “L’emploi des fluidifiants dans les BHP”, *Les bétons à hautes performances. Caractérisation, durabilité, applications*, Y. Malier (ed.), Presses Ponts et chaussées, Paris, 45-64.
- BAEL91 (2000), *Regulations for Conception, Calculation and Design of Reinforced Concrete Structures* (revised 99, DTVP 13-702), Paris (in French).
- Bairrão, R., Kačianauskas, R. and Kliukas, R. (2003), “Damage of high strength reinforced concrete columns under horizontal and vertical loading”, *Civil Engineering and Management*, **9**(3), 163-171.
- Bairrão, R., Kačianauskas, R. and Kliukas, R. (2003), “Local damage experimental research of high-strength concrete columns”, *Proc. of fib-Symposium Concrete Structures in Seismic Regions*, Athens, Greece, May.
- Bairrão, R., Duarte, R., Vaz, C. and Costa, A. (1995), “Portuguese methodology for the earthquake design of important structures”, *Proc. of the Second Int. Conf. on Seismology and Earthquake Engineering*, Teheran, Iran, May.
- Chung, D.D.L. (2002), “Improving cement-based materials using silica fume”, *J. Mater. Sci.*, **37**(4), 673-682.
- Conte, J.P. and Trombetti, T.L. (2000), “Linear dynamic modeling of a uniaxial servo-hydraulic shaking table system”, *Earthq. Eng. Struct. Dyn.*, **29**(9), 1375-1404.
- Crewe, A.J. and Severn, R.T. (2001), “The European collaborative programme on evaluating the performance of shaking tables”, *Philosophical Transactions of the Royal Society of London. Series A-Mathematical, Physical*

- and *Engineering Sciences*, **59**(1786), 1671-1696.
- Dong, Z. and Keru, W. (2001), "Fracture properties of high-strength concrete", *J. Mater. Civil Eng.*, **13**(1), 86-88.
- Duarte, R.T. (1994), "Development of shaking table testing techniques", *Report of Working Group 11, 10th European Conf. on Earthquake Engineering*, Vienna, Austria, August/September.
- Emílio, F.T., Duarte, R.T., Carvalhal, F.J., Costa, C.O., Vaz, C.T. and Corrêa, M.R. (1989), "The new LNEC shaking table for earthquake resistance testing", *Document LNEC-757*.
- FIP/CEP. (1990), "High strength concrete, State of the Art Report, SR 90/1", *Bulletin D'information*, 197.
- Flaga, K. (2000), "Advances in materials applied in civil engineering", *J. Mater. Proc. Tech.*, **106**, 173-183.
- Foster, S.J. (2001), "On behavior of high-strength concrete columns: Cover spalling, steel fibers, and ductility", *ACI Struct. J.*, **98**(4), 583-589.
- Hanganu, A.D., Onate, E. and Barbat, A.H. (2002), "A finite element methodology for local/global damage evolution in civil engineering structures", *Comput. Struct.*, **80**(20-21), 1667-1687.
- Heikal, M. and El-Didamony, H. (2000), "Effect of some superplasticizers on the properties of silica fume blended cement pastes", *Silicates Industriels*, **65**(11-12), 125-130.
- Kachanov, L.M. (1958), "On the creep fracture time", *Izv. AN SSSR*, **8**, 26-31 (in Russian).
- Khan, A.R., Al-Gadib, A.H. and Baluch, M.H. (1998), "An elasto damage constitutive model for high-strength concrete", R. de Borst (ed.), etc., *Computational Modeling of Concrete Structures*, 1, Balkema, Rotterdam, 133-142.
- Kmita, A. (2000), "A new generation of concrete in civil engineering", *J. Mater. Proc. Tech.*, **106**, 80-86.
- Labuz, F.J., Cattaneo, S. and Chen, L.H. (2001), "Acoustic emission at failure in quasi-brittle materials", *Construction and Building Materials*, **15**, 225-233.
- de Larrard, F. (1992), "Particules ultrafines pour l'élaboration des BTHP", *Les bétons à hautes performances. Caractérisation, durabilité, applications*, Y. Malier (ed.), Presses Ponts et Chaussées, Paris, 65-78.
- de Larrard, F. and Puch, C. (1992), "Formulation des BHP: la méthode des coulis", *Les bétons à hautes performances Caractérisation, durabilité, applications*, Y. Malier (ed.), Presses Ponts et Chaussées, Paris, 79-94.
- Lee, D.H. and Elnashai, A.S. (2002), "Inelastic seismic analysis of RC bridge piers including flexure-shear-axial interaction", *Struct. Eng. Mech.*, **13**(3), 241-260.
- Lemaitre, J. and Lipman, H. (1996), *Course of Damage Mechanics*, Springer, New-York.
- Li, Q., Zhang, L. and Ansari, F. (2002), "Damage constitutive for high strength concrete in triaxial cyclic compression", *Int. J. Solids Struct.*, **39**, 4013-4025.
- Lu, X. (1995), "Application of identification methodology to shaking table tests on reinforced concrete columns", *Eng. Struct.*, **17**(7), 505-511.
- Malier, Y. (1992), "L'utilisation du BHP dans une approche "système" de la construction", *Les bétons à hautes performances. Caractérisation, durabilité, applications*, Y. Malier (ed.), Presses Ponts et chaussées, Paris, 3-24.
- Manfredi, G. and Pecce, M. (1997), "Low cycle fatigue of RC beams in NSC and HSC", *Eng. Struct.*, **19**(3), 217-223.
- Minowa, C., Ogawa, N., Hayashida, T., Kogoma, I. and Okada, T. (1995), "Dynamic and static collapse tests of reinforced concrete columns", *Nuclear Engineering and Design*, **156**, 269-276.
- Murakami, S. and Kamiya, K. (1997), "Constitutive and damage evolution equations of elastic-brittle materials based on irreversible thermodynamics", *Int. J. Mech. Sci.*, **39**(4), 473-486.
- Ogawa, N., Ohtani, K., Katayama, T. and Shibata, H. (2001), "Construction of a three-dimensional, large-scale shaking table and development of core technology", *Philosophical Transactions of the Royal Society of London. Series A – Mathematical, Physical and Engineering Sciences*, **59**(1786), 1725-1751.
- Papa, E. and Taliercio, A. (1996), "Anisotropic damage model for the multiaxial static and fatigue behaviour of plain concrete", *Engng. Fracture Mech.*, **55**(2), 163-179.
- Paultre, P., Legeron, F. and Mongeau, D. (2001), "Influence of concrete strength and transverse reinforcement yield strength on behavior of high-strength concrete columns", *ACI Struct. J.*, **98**(4), 490-501.
- Suanno, R. and Ramm, E. (1994), "Analysis of three-dimensional reinforced concrete structures with coupling of plasticity and damage theories", Bažant Z.P. (ed.), etc., *Fracture and damage in quasi-brittle structures*, E&FN Spon, London, 519-532.

- Vadlūga, R., Kliukas, R. and Kudzys, A. (2000), "Influence of chemical additions on durability of vibrated and spun concrete under freezing and aggressive environment", *Fifth CANMET/ACI Int. Conf. on Durability of Concrete*, Barcelona, Spain, June, 403-412.
- Zhu, H., Li, L. and Wang D. (2003), "Damage assessment in periodic structures from measured natural frequencies by a sensitivity and transfer matrix-based method", *Struct. Eng. Mech.*, **16**(1), 17-34.